International Journal of Computer Applications (0975 - 8887)
Volume 184 - No.30, October 2022

An Experimental Comparative Study Between Machine Learning and Signal Processing Techniques to Detect Broken Rotors Bars in Induction Motors

Cleber Gustavo Dias
Informatics and Knowledge Management Graduate Program
Nove de Julho University - UNINOVE
São Paulo - Brazil

Rodrigo Cardozo de Jesus
Informatics and Knowledge Management Graduate Program
Nove de Julho University - UNINOVE
São Paulo - Brazil

ABSTRACT

This paper presents an experimental comparative study between some machine learning techniques and some signal processing methods to detect broken rotor bars in squirrel cage induction motors (SCIM). It has been used a current transformer to measure the stator current data from only one phase of the machine. The present research have addressed a common operational condition, particularly when motors run at low slip, i.e., with low load. In this work, three pre-processing approaches have been applied, such as the Fast Fourier Transform (FFT), Hilbert Transformation (HT) and some statistical data (SData). The sampled features have been applied to training and validating steps, by using three classification models, such as Support Vector Machine (SVM), k-Nearest Neighbor (KNN) and Logistic Regression (LR), not only to detect the failure, but also to evaluate its severity. The present study also presents a wide discussion about the parameters evaluated for each machine learning technique, in order to demonstrate that different choices can significantly affect the performance of each classifier. The best parameters have been identified for distinct rotor conditions. In addition, the Pearson correlation coefficient has been applied in a further investigation that shown the great possibility to reduce the number of input features and still maintaining a very good performance for the classifiers. The efficiency of this approach was evaluated and tested experimentally from a 7.5-kW induction motor running at low slip using a variable speed drive.

Keywords

Broken Rotor Bars, Fault Diagnosis, Machine Learning, Signal Processing, Induction Motor

1. INTRODUCTION

The Three-Phase Squirrel Cage Induction Motors (*SCIM*) are widely used in several applications and drives in the industry sector. Usually, this type of rotating machine is responsible for many energy conversion processes, particularly due to its reliability and robustness. In some countries, three-phase induction motors account for 30% to 80% of the total energy require for consumption [1]. Despite its robustness, the *SCIM* can be subjected to different kind of electrical and mechanical faults [2], during its startup and/or steady state operations, according to their load requirements and maintenance policy ([3] and [4]). As cited by other works [5], [6] and [7], the rotor faults represent around 10% of all failures, but when a broken bar occurs, for example, other parts of the machine may be damaged, which can cause machine downtime and production losses. In addition, rotor faults can cause unwanted effects such as vibrations, high temperature rises in the machine and the possibility of undermine its isolation, which reduces the service life machine. There are basically two types of approach to diagnose broken bars in *SCIM*, the invasive approach and non-invasive approach, as cited by [4]. A recent study, published by [8], for example, presents and summarizes some important researches and developments in the field of signal based automation for induction motor fault detection and diagnosis. That article has disclosed that motor current signature analysis (MCSA) method is still quite employed for broken rotor fault detection. Basically, this method uses Fast Fourier Transform to extract stator current features, as better described in the next section. A Hilbert Transform has the capacity of improving the MCSA approach, particularly for a SCIM running at very low slip, or low load conditions, as cited by [9] and [6]. Recently, other researchers have addressed the detection of broken bars, particularly for large machines, since these kind of motors usually operate at very low slip condition. In [10], for example, the authors have investigated broken rotor bars in a 3.15 MW induction motor. The aforementioned methods is a non-invasive approach, being substantially distinct from other works, such as the solutions presented by the works ([5] and [11]), since these techniques apply a Hall effect sensor installed near the air gap to measure magnetic disturbances according to the rotor condition. As mentioned by [12], a wide number of machine learning algorithms have been applied in the past years for motor fault diagnosis [13] and [14], using both frequency and time-domain signals as input data, but the performance of classifiers, for example, is very heterogeneous. Therefore, the present research has been carried out using FFT and HT methods as digital signal processing methods, statistical data extracted from the stator current in the time-domain and three of the most known classifiers, usually found in the rotating electrical machine monitoring field. The combination of the best parameters of each classifier and the signal processing of the stator current have been carefully

investigated. In the next section the data preprocessing methods are presented and discussed.

2. DATA PREPROCESSING: DIGITAL SIGNAL PROCESSING METHODS FOR STATOR CURRENT FEATURES EXTRACTION

As described in the previous section, a lot of studies have invested efforts to applying digital signal processing methods, in order to extract relevant features from signals measured and/or estimated in induction motors. Among the best known and most used approaches, there are those that make use of frequency domain and time domain algorithms, as disclosed by the works published in [5], [15] and [16]. In the present work, three stator current feature extraction methods have been used such as FFT, HT and statistics metrics. The following subsections detail the fundamentals of each one.

2.1 Fast Fourier Transform Approach for Stator Current Feature Extraction

The FFT approach has been widely used in the condition monitoring of induction motor during the last decades. More particularly, for broken rotor bars detection there are sideband frequencies (left and right) around the fundamental one in case of the occurrence of this kind of fault. In addition, the amplitude of the sideband indicates the severity of the failure, i.e., the number of broken bars, for example in [7].

$$f_{BRB} = (1 \pm 2ks)fs \tag{1}$$

Where f_{BRB} represents the broken bar frequency (fault frequency), fs is the fundamental frequency, s is the slip and k is a constant related to the number of the harmonic.

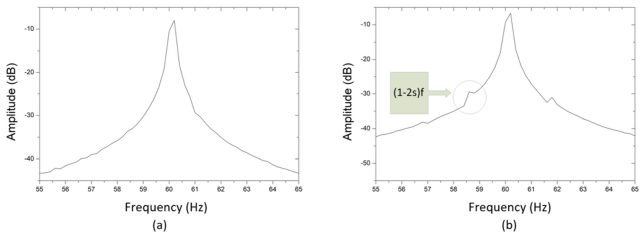

Fig. 1: Left side band frequency (1-2s)f, after applying FFT in the stator current, according to a) a health motor (without broken rotor bars) and b) motor with one broken bar running at slip of 0.66%.

As shown in Figure 1, a particular fault frequency near the fundamental one is shown for a damaged rotor (broken bars). Therefore, when a rotor failure occurs the fault frequency, its amplitude and the slip are computed to use as inputs to a machine learning classifier as better described in section 4. The input vector using these features is constructed as:

$$FFT(features) = [FFreq, AFFreq, Slip] \tag{2}$$

Where FFreq is the fault frequency in Hz, AFFreq is the amplitude of the fault frequency in dB and Slip is the slip (s) of the rotor shaft in percentage. This input vector is used to evaluate some machine learning performances for an induction motor running at very low slip conditions, as better described in section IV. At low slip operational conditions it is very difficult do identify this kind of rotor fault using FFT, as disclosed by numerous works ([5], [7], [11],[17], [18] and [19]). However, this kind of frequency-domain approach is current widely used in broken rotor bars diagnosis.

2.2 Hilbert Transform for Stator Current Feature Extraction

As described by Ref. [20], the Hilbert Transform (HT) can be applied as an efficient technique for signal demodulation and for harmonic components extraction from a time domain signal. In the past years, some authors ([6], [7], [9] and [21]) have implemented HT for broken bars detection in distinct load conditions. By considering a $x(t)$ time-domain signal, such as one phase of the stator current, the HT can be defined as follows (Equation 3):

$$HT(x(t)) = y(t) = \frac{1}{\pi}\int_{-\infty}^{+\infty} x(\tau)\frac{1}{t-\tau}, d\tau \tag{3}$$

In the present work the so-called analytical signal is used $\overrightarrow{x(t)}$ according to Equation 4:

$$\overrightarrow{x(t)} = x(t) + jy(t) = b(t)e^{j\theta(t)} \tag{4}$$

After calculating the Hilbert modulus of $\overrightarrow{x(t)}$, the FFT is applied to extract a new fault frequency (2sf), according to the failure in the rotor cage. In this approach, the frequencies to be detected are very low, as cited by works [6] and [7]. This fault frequency component is shown in Figure 2.

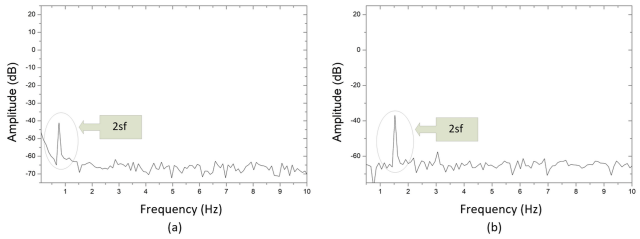

Fig. 2: Left side band frequency (2sf), after applying HT+FFT in the Hilbert modulus, according to one broken bar for a) motor running at slip of 1.15% and b) motor running at slip of 0.66%.

In this case, a second input vector was obtained according to Equation 5.

$$HTFT(features) = [HTFreq, AHTFreq, Slip] \tag{5}$$

Where HTFreq is the fault frequency (2sf) in Hz, AHTFreq is the amplitude of the fault frequency in dB and Slip is the slip (s) of the rotor shaft in percentage.

2.3 Statistical Approach for Stator Current Feature Extraction

The use of statistical features, particularly extracted from some motor time-domain signals, were investigated by researchers to detect broken rotor bars in induction motors recently ([5], [22] and [23]). In [5], for example, some time domain statistical features were extracted from a Hall effect sensor installed between two stator slots

Table 1. : Statistical Features [22]

Feature	Description	Equation
STAT1	Standard Deviation	$\sigma = \frac{\sum(x_i-\bar{x})^2}{n-1}$
STAT2	Mean	$m_1 = \frac{1}{n}\sum(x)$
STAT3	Variance	$m_2 = \frac{1}{n}\sum(x_i-\bar{x})^2$
STAT4	3^{er} Order Moment	$m_3 = \frac{1}{n}\sum(x_i-\bar{x})^3$
STAT5	4^{th} Order Moment	$m_4 = \frac{1}{n}\sum(x_i-\bar{x})^4$
STAT6	6^{th} Order Moment	$m_6 = \frac{1}{(n\times m_2)\sum(x_i-\bar{x})^6}$
STAT7	1^{st} Order Cumulant	$c_1 = m_1$
STAT8	2^{nd} Order Cumulant	$c_2 = m_2 - m1^2$
STAT9	3^{er} Order Cumulant	$c_3 = m_3 - 3m1m2 + 2m_1^3$
STAT10	4^{th} Order Cumulant	$c_4 = m_4 + m3m1 - 3m2^2 + 12m2^2 - 6m1^4$
STAT11	Skewness	$skew = \frac{m_3}{(\sqrt{m_2})^3}$
STAT12	Absolute mean	$\|\bar{x}\| = \frac{1}{n}\sum\|x\|$
STAT13	Maximum Peak Value	$x_p = max\|x\|$
STAT14	Square Root Value	$x_r = (\frac{1}{n}\sum\sqrt{\|x\|})^2$
STAT15	Crest Factor	$f_c = \frac{x_p}{x_{rms}}$
STAT16	Shape Factor	$f_o = \frac{x_{rms}}{\|x\|}$
STAT17	Root Mean Square	$x_{rms} = \sqrt{\frac{1}{n}\sum(x_i-\bar{x})^2}$

of the machine, in order to detect broken rotor bars. In the present work, it has been evaluated the use of some statistical metrics calculated from the stator current, as proposed by [22] (Table 1). Therefore, the FFT and HT approaches, detailed in subsections 2.1 and 2.2, are frequency-domain methods and the aforementioned statistical features are extracted from the one phase of the stator current, considering its time-domain waveform, as suggested by [22]. Thus, on each stator current sample, the 17 statistical features are calculated and the third input vector is obtained, such as described in Equation 6.

$$STAT(features) = [STAT1, .., STAT17] \quad (6)$$

The next section explain the machine learning techniques and its main parameters explored in the present research.

3. THE MACHINE LEARNING TECHNIQUES FOR BROKEN ROTOR BARS CLASSIFICATION

In this work, three classifiers have been implemented and tested for broken rotor bars detection and for rotor failure severity evaluation. They are described as follows.

3.1 Logistic Regression (RL)

In general, a logistic regression is a popular machine learning technique used when the dependent variable is categorical. In this work, the logistic regression is applied for a multiclass classification, i.e., its output depends on the number of the rotor broken bars. As cited by [24], it is important to mention that logistic regression is a relatively simple method that works similarly to a linear regression, except to the output values. According to the kind of problem, some approaches are used to solve an optimization problem and specific solvers could be implemented such as 'newton-cg', 'sag', 'saga' and lbfgs. In this case, only these solvers handle multinomial loss.

3.2 Support Vector Machine (SVM)

This kind of classifier is known as a statistical model and applies an optimization problem to find the best hyperplane that separates most the target classes ([25] and [26]) . In the present research the cost tuning and gamma parameters have been tested using a Radial Basis Function (RBF) or Gaussian Kernel. This type of kernel function has been chosen due to its good performance disclosed in [5].

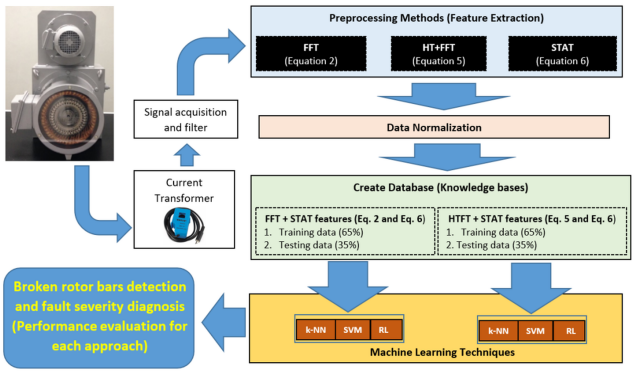

Fig. 3: Proposed Methodology

Table 2. : Preprocessing methods and features extracted from stator current of the SCIM

Method	Extracted features	Total Features
FFT	Equation (2)	3
HT+FFT	Equation (5)	3
Statistical features	Equation (6)	17

3.3 K-Nearest Neigbor (KNN)

In general, the main parameters of a KNN classifer are the distance metric and the number of neighbors (Nb). This kind of machine learning algorithm is a nonparametric method and, as cited by [5], it assigns each unlabeled pattern to the cluster of its nearest labeled neighbors. In the present research, Nb varies from 1 to 9 and two distance metrics have been evaluated, namely Minkowski and Euclidean.

4. METHODOLOGY FOR FEATURE SELECTION AND BROKEN BARS DETECTION

As shown in the previous sections, three signal preprocessing methods and three machine learning techniques have been investigated to extract the features from the stator current and for broken bars detection. In Table 2, the processing methods and their features are presented and Table 3 shows the machine learning techniques and their parameters evaluated on each case. In Figure 3 it is possible to note the main steps of the present research. It should be noted that all algorithms have been implemented in the Python software and some libraries have been used for mathematics and machine learning purposes, such as "numpy", "pandas", "matplotlib", "sklearn" and "scipy". As described by [25], the performance metrics used for designing a classifier are as follows: i-) Accuracy; ii-) Precision; iii-) Recall; and iv-) F1-scored. These metrics are able to evaluate the true and false indications related to the rotor structure condition monitoring, as better described in Section VI.

5. EXPERIMENTAL SETUP

The experimental tests has been carried out in laboratory, using an induction motor 7.5 kW, four poles, 60 Hz and 38 rotor bars. This motor has a rated slip in 3.4%. The rotor structure is composed by bolts and nuts being possible to simulate different numbers of broken bars. It should be mentioned that the cited motor has been particularly manufactured to research purposes and simulate a rotor bar failure with the end-ring section, as shown in Figure 4.

Table 3. : Machine learning techniques and parameters tested for broken rotor bars detection

Technique	Parameters
Logistic Regression (RL)	Solver type (newton-cg, sag, saga and lbfgs) and C-value
Support Vector Machine (SVM)	Cost tuning parameter ("C") and gamma (g), using Radial Basis Function (RBF) kernel
K-Nearest Neighborhood (KNN)	Number of neighbors (Nb) and distance metrics (Dm)

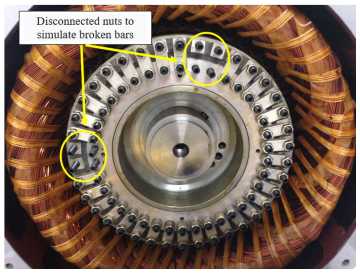

Fig. 4: Rotor structure with bolts and nuts to simulate broken rotor bars

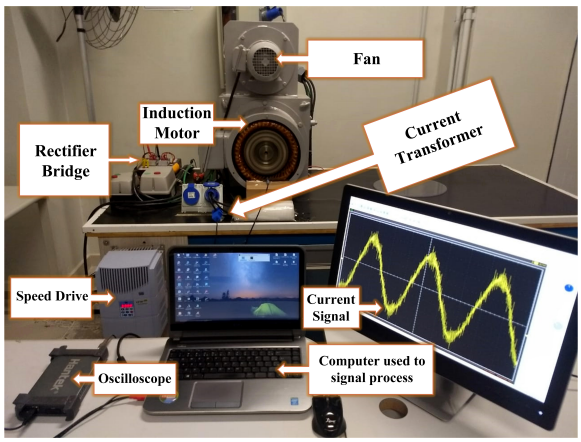

Fig. 5: Apparatus setup used for experimental tests

The experimental test bench is shown in Figure 6. The stator current has been measured using a current transformer (20A/1V) and data have been sampled using a digital Oscilloscope Hantek (HT6022BE), with bandwith in 20 MHz and a sample frequency in 10kHz. The current data have been stored in a PC computer. It should be mentioned that the induction motor has an internal braking system (Foucault brake), which is possible to apply different mechanical loads in the rotor shaft. The machine was driven by a frequency inverter (speed drive).

6. RESULTS AND DISCUSSION

This section shows the experimental results and the rotor fault detection according to the proposed methodology. Firstly, it should me mentioned the features and the data-set built for stator current data processing and failure detection. As shown in Table 2, the first data-set has prepared using 20 extracted features (equation2 and equation 6) and the second data-set also has 20 extracted features (equation 5 and equation 6). As cited by [22], the combination of statistical features with frequency domain features can increase the classifier efficiency. In the present research, as shown in Table 4, the data-set has been implemented for 5 classes, i.e., considering the output of each classifier with the following conditions: i) a health rotor (class = 0); ii) one broken bar (class = 1); iii) two broken bars (class = 2); iv) three broken bars (class = 3); and v) four broken bars (class = 4). It is important to highlight that the experimental tests have been carried out for the induction motor running at very low slip in a range from 0.66% to 1.16%. The rated slip of the tested motor is around 3.4%.

6.1 The rotor fault diagnosis results using FFT+STAT approach as feature extraction method for classifier inputs

In the present case, the stator current features were extracted using the Fast Fourier transform of the stator current and the statistical features processed during 10s as a window sample time. A total of 20 features have been applied as inputs for each classifier, as described in Table 2. In Table 4 the data-set has been described for classifier learning and testing purposes. The FFT+STAT features has been tested using RL, KNN and SVM classifiers and the results for each one are described in the next subsections.

6.1.1 Results obtained for a RL classifier. The RL classifier performance has been investigated for different configurations as shown in Table 5. In general, as can be seen, the solver type did not directly influence the performance, but the C-value was the parameter which was able to improve the precision, recall and accuracy of the RL classifier for each rotor condition. The C-value equal to 0.16 has achieved the best accuracy (0.5166) for a healthy rotor and for 1BB, 2BB and 3BB. Though C-value of 0.0016 has shown a good performance for a 4BB rotor condition, this parameter value indicated the worst performance compared to the other rotor fault cases.

6.1.2 Results obtained for a KNN classifier. As the previous case, in this approach the input features have been extracted using FFT+STAT and applying a KNN classifier. The number of neighbors (Nb) and distance metrics have been tested in distinct configurations as shown in Table 6. As can be noted, the number of neighbors equal to 7 has demonstrated the best performance, considering the accuracy (accuracy = 0.6880), regardless the distance metric. However, the authors have tested other distance metrics and Chebyshev, for example, have shown a general underperforming when compared to the use of Euclidean and Minkowski approaches. Anyway, the worst result using KNN classifier (accuracy = 0.6559) is better when compared to RL classifier (accuracy = 0.5166). This result has achieved some findings:i-) this second approach has been able to distinguish more between a fault rotor when compared to the classifier model using RL, avoiding, for example, more false positive indications; and ii-) the KNN classifier has been able to identify and distinguish the number of broken bars compared to the previous solution.

6.1.3 Results obtained for a SVM classifier. In this item a SVM classifier has been also tested considering distinct parameters. As described in Table 3, the cost tuning parameter (C) value and gamma (g) have been investigated applying a Radial Basis Function kernel (RBF). In Table 7 it is possible to observer that the best accuracy values are a little better then those obtained using a KNN classifier. In this case, the values of C = 1 and g = 0.50 (or g = 0.25) have disclosed a better configuration. Thus, when compared to the other classifiers (RL and KNN), the SVM has demonstrated a bet-

Table 4. : Data-set used for evaluation of the best classifier parameters and rotor fault detection

Machine learning operation	Total of experiments	Number of experiments per slip [slip(Qtde)]	Number of experiments per class
Learning data	1560 (65%)	[s=0.5%(375)] [s=0.66% (398)] [s=1%(396)] [s=1.16%(391)]	312 (5 classes)
Testing data	840 (35%)	[s=0.5%(225)] [s=0.66% (202)] [s=1%(204)] [s=1.16%(209)] (65%)	168 (5 classes)
Total	2400	2400	2400

Table 5. : RL classifier performance using distinct configurations and FFT+STAT input features

RL Configuration	Precision/Recall/ F1-score(Healthy rotor)	Precision/Recall/ F1-score(1BB)	Precision/Recall/ F1-score(2BB)	Precision/Recall/ F1-score(3BB)	Precision/Recall/ F1-score(4BB)	**Accuracy**
Newton-cg solver and Cs = 1.6	0.5362 / 0.6607 / 0.592	0.3960 / 0.4762 / 0.4324	0.3846 / 0.2976 / 0.3355	0.6829 / 0.5 / 0.5773	0.5898 / 0.625 / 0.6069	0.5119
Newton-cg solver and Cs = 0.16	0.5432 / 0.6726 / 0.6010	0.3913 / 0.4821 / 0.432	0.3983 / 0.2916 / 0.3367	0.6774 / 0.5 / 0.5733	0.6011 / 0.6369 / 0.6185	0.5166
Newton-cg solver and Cs = 0.016	0.5427 / 0.6428 / 0.5885	0.3607 / 0.4702 / 0.4082	0.3913 / 0.2678 / 0.3180	0.688 / 0.5119 / 0.5870	0.6043 / 0.6547 / 0.6285	0.5095
Newton-cg solver and Cs = 0.0016	0.5127 / 0.6012 / 0.5534	0.3262 / 0.4583 / 0.3811	0.2380 / 0.089 / 0.1298	0.5918 / 0.5178 / 0.5523	0.5939 / 0.6964 / 0.6410	0.4726
Sag solver and Cs = 1.6	0.5362 / 0.6607 / 0.592	0.3960 / 0.4762 / 0.4324	0.3846 / 0.2976 / 0.3355	0.6829 / 0.5 / 0.5773	0.5898 / 0.625 / 0.6069	0.5119
Sag solver and Cs = 0.16	0.5432 / 0.6726 / 0.6010	0.3913 / 0.4821 / 0.432	0.3983 / 0.2916 / 0.3367	0.6774 / 0.5 / 0.5733	0.6011 / 0.6369 / 0.6185	0.5166
Sag solver and Cs = 0.016	0.5427 / 0.6428 / 0.5885	0.3607 / 0.4702 / 0.4082	0.3913 / 0.2678 / 0.3180	0.688 / 0.5119 / 0.5870	0.6043 / 0.6547 / 0.6285	0.5095
Sag solver and Cs = 0.0016	0.5127 / 0.6012 / 0.5534	0.3262 / 0.4583 / 0.3811	0.2380 / 0.089 / 0.1298	0.5918 / 0.5178 / 0.5523	0.5939 / 0.6964 / 0.6410	0.4726
Saga solver and Cs = 1.6	0.5362 / 0.6607 / 0.592	0.3960 / 0.4762 / 0.4324	0.3846 / 0.2976 / 0.3355	0.6829 / 0.5 / 0.5773	0.5898 / 0.625 / 0.6069	0.5119
Saga solver and Cs = 0.16	0.5432 / 0.6726 / 0.6010	0.3913 / 0.4821 / 0.432	0.3983 / 0.2916 / 0.3367	0.6774 / 0.5 / 0.5733	0.6011 / 0.6369 / 0.6185	0.5166
Saga solver and Cs = 0.016	0.5427 / 0.6428 / 0.5885	0.3607 / 0.4702 / 0.4082	0.3913 / 0.2678 / 0.3180	0.688 / 0.5119 / 0.5870	0.6043 / 0.6547 / 0.6285	0.5095
Saga solver and Cs = 0.0016	0.5127 / 0.6012 / 0.5534	0.3262 / 0.4583 / 0.3811	0.2380 / 0.089 / 0.1298	0.5918 / 0.5178 / 0.5523	0.5939 / 0.6964 / 0.6410	0.4726
Lbfgs solver and Cs = 1.6	0.5362 / 0.6607 / 0.592	0.3960 / 0.4762 / 0.4324	0.3846 / 0.2976 / 0.3355	0.6829 / 0.5 / 0.5773	0.5898 / 0.625 / 0.6069	0.5119
Lbfgs solver and Cs = 0.16	0.5432 / 0.6726 / 0.6010	0.3913 / 0.4821 / 0.432	0.3983 / 0.2916 / 0.3367	0.6774 / 0.5 / 0.5733	0.6011 / 0.6369 / 0.6185	0.5166
Lbfgs solver and Cs = 0.016	0.5427 / 0.6428 / 0.5885	0.3607 / 0.4702 / 0.4082	0.3913 / 0.2678 / 0.3180	0.688 / 0.5119 / 0.5870	0.6043 / 0.6547 / 0.6285	0.5095
Lbfgs solver and Cs = 0.0016	0.5127 / 0.6012 / 0.5534	0.3262 / 0.4583 / 0.3811	0.2380 / 0.089 / 0.1298	0.5918 / 0.5178 / 0.5523	0.5939 / 0.6964 / 0.6410	0.4726

ter accuracy as shown in Tables 5, 6 and 7. Therefore, SVM has shown the possibility to avoid false alarms (negative and positive indications) considering the best parameters.

6.2 The rotor fault diagnosis results using HTFT+STAT approach as feature extraction method for classifier inputs

In the present case, the stator current features were extracted using the Hilbert and Fast Fourier transform of the stator current and the statistical features processed during 10s as a window sample time. A total of 20 features have also been applied as inputs for each classifier, as described in Table 3. The data-set, i.e, the number of experiments, is the same used for the FFT+STAT approach. The HTFT+STAT features has been tested using RL, KNN and SVM classifiers and the results for each one are described in the next subsections.

6.2.1 Results obtained for a RL classifier. In Table 8 it is possible to observe that, regardless the solver type, Cs parameter set in 1.6 has achieved the best accuracy (accuracy around 0.64). It should be noted that the mentioned accuracy is better than that found for a RL classifier using only the FFT+STAT approach (best accuracy around 0.5166) for feature extraction. In addition, the present results are quite near those obtained using KNN classifier and FFT+STAT input features (Table 6). This approach has a great capacity to differentiate between a rotor fault and a healthy one, although the severity identification is quite complicated, particularly between 2BB and 3BB conditions. This finding can be observed using the precision, recall and F1-score values in Table 8, for example. Thus, the use of Hilbert and FFT approach, as a signal processing method to extract stator current features, has improved the rotor diagnosis efficiency, when compared to the use of FFT+STAT and the same RL classifier parameters.

6.2.2 Results obtained for a KNN classifier. In this case, KNN has been applied as a classifier using HTFT+STAT for feature extraction. Table 9 disclosed a better accuracy (0.8190) when compared to the same classifier using only FFT+STAT input features (Table 6). Moreover, regardless the distance metric (Euclidean or Minkowski) used on each configuration, the Nb parameter adjusted in a value of 5 has achieved the best accuracy results (0.8190) for rotor condition evaluation.

6.2.3 Results obtained for a SVM classifier. In this approach, the SVM classifier has been tested using distinct configurations, as cited in section 6.1.3. However, the inputs have been investigated using HTFT+STAT features and the accuracy (Table 10) results have shown better results when compared to any previous configuration (accuracy around 0.8464). It is interesting to observe that, using FFT+STAT input features the best SVM configuration was found for C = 1 and g = 0.50 (or g = 0.25), but in the present case the best SVM parameters are C = 100 and g=0.25 (or g = 0.50). In this case, is possible to avoid false positive indications for rotor condition evaluation and this kind of configuration, using HTFT+STAT input features and a SVM classifier, shows better results when compared to all previous cases.

6.3 The use of the Pearson correlation coefficient for stator feature selection

As mentioned before, this research has also investigated the use of Pearson correlation coefficient (PCC) to select some stator features as inputs for each classifier. By using a heat map, it is possible to evaluate the strength of each variable, i.e, considering each feature and the output. Since the HTFT+STAT features have demonstrated a better result when compared to the use of only FFT, the Pearson correlation has been discussed using Hilbert and statistical features. The Pearson coefficient can take a range of values from +1 to -1 and a value of 0 indicates that there is no association between the two variables (input feature and output). As cited by [27] and [28], the PCC is able to screened more information from data. A several reduction scenarios have been tested in the present research, but the use of the first 8 variables (positive correlation) and 2 variables with more negative correlations (highlighted in a red square) shown the best accuracy results for rotor condition evaluation. However, the SVM classifier still showed best accuracy results are shown in Table 11. Figure 6 shows a ROC curves using features extracted after applying PCC. It is interesting to observe that the use of re-

Table 6. : KNN classifier performance using distinct configurations and FFT+STAT input features

KNN Configuration	Precision/Recall/ F1-score(Healthy rotor)	Precision/Recall/ F1-score(1BB)	Precision/Recall/ F1-score(2BB)	Precision/Recall/ F1-score(3BB)	Precision/Recall/ F1-score(4BB)	**Accuracy**
Euclidean and Nb = 1	0.7117 / 0.7202 / 0.7159	0.6176 / 0.625 / 0.6213	0.5379 / 0.5059 / 0.5214	0.64 / 0.6666 / 0.6530	0.7664 / 0.7619 / 0.7641	0.6559
Euclidean and Nb = 3	0.7225 / 0.7440 / 0.7331	0.6 / 0.6071 / 0.6035	0.5286 / 0.4940 / 0.5107	0.6647 / 0.6964 / 0.6802	0.7865 / 0.7678 / 0.7771	0.6619
Euclidean and Nb = 5	0.7209 / 0.7380 / 0.7294	0.6265 / 0.6190 / 0.6227	0.5476 / 0.5476 / 0.5476	0.6483 / 0.7023 / 0.6742	0.7960 / 0.7202 / 0.7562	0.6654
Euclidean and Nb = 7	0.7622 / 0.7440 / 0.7530	0.6333 / 0.6785 / 0.6551	0.5647 / 0.5714 / 0.5680	0.6946 / 0.6904 / 0.6925	0.7987 / 0.756 / 0.7767	0.6880
Euclidean and Nb = 9	0.7530 / 0.7440 / 0.7485	0.6145 / 0.6547 / 0.6340	0.5523 / 0.5654 / 0.5588	0.7083 / 0.7083 / 0.7083	0.8258 / 0.7619 / 0.7925	0.6869
Minkowski and Nb = 1	0.7117 / 0.7202 / 0.7159	0.6176 / 0.625 / 0.6213	0.5379 / 0.5059 / 0.5214	0.64 / 0.6666 / 0.6530	0.7664 / 0.7619 / 0.7641	0.6559
Minkowski and Nb = 3	0.7225 / 0.7440 / 0.7331	0.6 / 0.6071 / 0.6035	0.5286 / 0.4940 / 0.5107	0.6647 / 0.6964 / 0.6802	0.7865 / 0.7678 / 0.7771	0.6619
Minkowski and Nb = 5	0.7209 / 0.7380 / 0.7294	0.6265 / 0.6190 / 0.6227	0.5476 / 0.5476 / 0.5476	0.6483 / 0.7023 / 0.6742	0.7960 / 0.7202 / 0.7562	0.6654
Minkowski and Nb = 7	0.7622 / 0.7440 / 0.7530	0.6333 / 0.6785 / 0.6551	0.5647 / 0.5714 / 0.5680	0.6946 / 0.6904 / 0.6925	0.7987 / 0.756 / 0.7767	0.6880
Minkowski and Nb = 9	0.7530 / 0.7440 / 0.7485	0.6145 / 0.6547 / 0.6340	0.5523 / 0.5654 / 0.5588	0.7083 / 0.7083 / 0.7083	0.8258 / 0.7619 / 0.7925	0.6869

Table 7. : SVM classifier performance using distinct configurations and FFT+STAT input features

SVM Configuration	Precision/Recall/ F1-score(Healthy rotor)	Precision/Recall/ F1-score(1BB)	Precision/Recall/ F1-score(2BB)	Precision/Recall/ F1-score(3BB)	Precision/Recall/ F1-score(4BB)	**Accuracy**
C = 1 and g = 0.0025	0.9859 / 0.4166 / 0.5857	0.2996 / 0.5833 / 0.3959	0.3212 / 0.3690 / 0.3435	0.7383 / 0.4702 / 0.5745	0.7183 / 0.6071 / 0.6580	0.4892
C = 1 and g = 0.25	0.7588 / 0.7678 / 0.7633	0.6419 / 0.619 / 0.6303	0.5579 / 0.6309 / 0.5921	0.7302 / 0.6607 / 0.6937	0.7951 / 0.7857 / 0.7904	0.6928
C = 1 and g = 0.50	0.7337 / 0.7380 / 0.7359	0.6583 / 0.6309 / 0.6443	0.581/ 0.619 / 0.5994	0.7116 / 0.6904 / 0.7009	0.7916 / 0.7916 / 0.7916	0.6940
C = 100 and g = 0.0025	0.7239 / 0.7023 / 0.713	0.4972 / 0.5297 / 0.5129	0.4088 / 0.5476 / 0.4682	0.7843 / 0.4762 / 0.5925	0.7309 / 0.7440 / 0.7374	0.6
C = 100 and g = 0.25	0.6614 / 0.756 / 0.7055	0.6121 / 0.6012 / 0.6066	0.5411 / 0.5476 / 0.5443	0.6484 / 0.6369 / 0.6426	0.8378 / 0.7380 / 0.7848	0.656
C = 100 and g = 0.50	0.6815 / 0.7261 / 0.7031	0.6234/ 0.6012 / 0.6121	0.52 / 0.5416 / 0.5306	0.6667 / 0.6547 / 0.6606	0.8427 / 0.7976 / 0.8195	0.6643
C = 200 and g = 0.0025	0.7219 / 0.7262 / 0.7240	0.4971 / 0.5238 / 0.5101	0.4318 / 0.5654 / 0.4897	0.7663 / 0.488 / 0.5963	0.7365 / 0.7321 / 0.7343	0.6071
C = 200 and g = 0.25	0.6756 / 0.7440 / 0.7082	0.5955 / 0.6309 / 0.6127	0.5460 / 0.5297 / 0.5377	0.6407 / 0.6369 / 0.6388	0.8367 / 0.7321 / 0.7809	0.6547
C = 200 and g = 0.50	0.6910 / 0.7321 / 0.7109	0.6 / 0.5892 / 0.5946	0.52 / 0.5416 / 0.5306	0.6606 / 0.6488 / 0.6546	0.8471 / 0.7916 / 0.8184	0.6607
C = 300 and g = 0.0025	0.6949 / 0.7321 / 0.7130	0.5060 / 0.494 / 0.5	0.4208 / 0.5535 / 0.4781	0.7798 / 0.5059 / 0.6137	0.7337 / 0.7380 / 0.7359	0.6047
C = 300 and g = 0.25	0.6684 / 0.7321 / 0.6988	0.5847 / 0.5952 / 0.5899	0.5083 / 0.5416 / 0.5244	0.6441 / 0.625 / 0.6344	0.8531 / 0.7261 / 0.7845	0.6440
C = 300 and g = 0.50	0.6871 / 0.7321 / 0.7089	0.6073 / 0.5892 / 0.5981	0.5170 / 0.5416 / 0.5290	0.6606 / 0.6488 / 0.6546	0.8471 / 0.7916 / 0.8184	0.6607

Table 8. : RL classifier performance using distinct configurations and HTFT+STAT input features

RL Configuration	Precision/Recall/ F1-score(Healthy rotor)	Precision/Recall/ F1-score(1BB)	Precision/Recall/ F1-score(2BB)	Precision/Recall/ F1-score(3BB)	Precision/Recall/ F1-score(4BB)	**Accuracy**
Newton-cg solver and Cs = 1.6	0.9314 / 0.9702 / 0.9504	0524 / 0.06488 / 0.5797	0.3841 / 0.3452 / 0.3636	0.6397 / 0.5178 / 0.5723	0.7353 / 0.744 / 0.7396	0.6452
Newton-cg solver and Cs = 0.16	0.9044 / 0.9583 / 0.9306	0.505 / 0.5952 / 0.5464	0.3947 / 0.3571 / 0.375	0.6304 / 0.5178 / 0.5686	0.7299 / 0.756 / 0.7427	0.6369
Newton-cg solver and Cs = 0.016	0.8077 / 0.875 / 0.84	0.4398 / 0.5654 / 0.4948	0.4298 / 0.2916 / 0.3475	0.6124 / 0.5178 / 0.5649	0.6914 / 0.7738 / 0.7303	0.6047
Newton-cg solver and Cs = 0.0016	0.6271 / 0.6607 / 0.6434	0.3788 / 0.5119 / 0.4354	0.4090 / 0.1607 / 0.2307	0.55 / 0.5238 / 0.5365	0.6238 / 0.7797 / 0.6931	0.5274
Sag solver and Cs = 1.6	0.8846 / 0.9583 / 0.92	0.5151 / 0.6071 / 0.5573	0.4013 / 0.3630 / 0.3812	0.6397 / 0.5178 / 0.5723	0.7441 / 0.7619 / 0.7529	0.6416
Sag solver and Cs = 0.16	0.8833 / 0.9464 / 0.9138	0.505 / 0.6012 / 0.5489	0.3959 / 0.3512 / 0.3722	0.6304 / 0.5178 / 0.5686	0.7341 / 0.756 / 0.7448	0.6345
Sag solver and Cs = 0.016	0.8077 / 0.875 / 0.84	0.4398 / 0.5654 / 0.4948	0.4298 / 0.2916 / 0.3475	0.6214 / 0.5178 / 0.5649	0.6914 / 0.7738 / 0.7303	0.6047
Sag solver and Cs = 0.0016	0.6271 / 0.6607 / 0.6434	0.3788 / 0.5119 / 0.4354	0.4090 / 0.1607 / 0.2307	0.55 / 0.5238 / 0.5365	0.6238 / 0.7797 / 0.6931	0.5273
Saga solver and Cs = 1.6	0.8449 / 0.9404 / 0.8901	0.4925 / 0.5892 / 0.5365	0.3943 / 0.3333 / 0.3613	0.6350 / 0.5178 / 0.5704	0.7341 / 0.7559 / 0.7448	0.6274
Saga solver and Cs = 0.16	0.8449 / 0.9404 / 0.8901	0.4901 / 0.5952 / 0.5376	0.3956 / 0.3273 / 0.3583	0.6397 / 0.5178 / 0.5723	0.7298 / 0.7559 / 0.7427	0.6274
Saga solver and Cs = 0.016	0.8066 / 0.8690 / 0.8366	0.4377 / 0.5654 / 0.4935	0.4298 / 0.2916 / 0.3475	0.6214 / 0.5178 / 0.5649	0.6914 / 0.7738 / 0.7303	0.6035
Saga solver and Cs = 0.0016	0.6166 / 0.6607 / 0.6379	0.3788 / 0.5119 / 0.4354	0.4127 / 0.1547 / 0.2251	0.5528 / 0.5297 / 0.5410	0.6267 / 0.7797 / 0.6949	0.5274
Lbfgs solver and Cs = 1.6	0.9314 / 0.9702 / 0.9504	0.5240 / 0.6488 / 0.5797	0.3815 / 0.3452 / 0.3625	0.6397 / 0.5178 / 0.5723	0.7396 / 0.7440 / 0.7418	0.6452
Lbfgs solver and Cs = 0.016	0.8077 / 0.875 / 0.84	0.4398 / 0.5654 / 0.4948	0.4298 / 0.2916 / 0.3475	0.6214 / 0.5178 / 0.5649	0.6914 / 0.7738 / 0.7303	0.6047
Lbfgs solver and Cs = 0.0016	0.6271 / 0.6607 / 0.6434	0.3788 / 0.5119 / 0.4354	0.4090 / 0.1607 / 0.2307	0.55 / 0.5238 / 0.5365	0.6238 / 0.7797 / 0.6931	0.5273

Table 9. : KNN classifier performance using distinct configurations and HTFT+STAT input features

KNN Configuration	Precision/Recall/ F1-score(Healthy rotor)	Precision/Recall/ F1-score(1BB)	Precision/Recall/ F1-score(2BB)	Precision/Recall/ F1-score(3BB)	Precision/Recall/ F1-score(4BB)	**Accuracy**
Euclidean and Nb = 1	0.9743 / 0.9047 / 0.9382	0.7237 / 0.7797 / 0.7507	0.7106 / 0.6726 / 0.6911	0.7371 / 0.7678 / 0.7521	0.8639 / 0.8690 / 0.8664	0.7988
Euclidean and Nb = 3	0.9697 / 0.9523 / 0.9609	0.7633 / 0.7678 / 0.7655	0.7361 / 0.7142 / 0.7250	0.7307 / 0.7916 / 0.76	0.8695 / 0.8333 / 0.8510	0.8119
Euclidean and Nb = 5	0.9636 / 0.9464 / 0.9549	0.7927 / 0.7738 / 0.7831	0.7613/ 0.7023 / 0.7306	0.7157 / 0.8095 / 0.7597	0.8734 / 0.8630 / 0.8682	0.8190
Euclidean and Nb = 7	0.9634 / 0.9404 / 0.9518	0.7572 / 0.7797 / 0.7683	0.7516 / 0.7023 / 0.7261	0.7311 / 0.8095 / 0.7683	0.8812 / 0.8392 / 0.8597	0.8143
Euclidean and Nb = 9	0.9461 / 0.9404 / 0.9432	0.7485 / 0.7440 / 0.7462	0.7134 / 0.6964 / 0.7048	0.7189 / 0.7916 / 0.7535	0.8789 / 0.8214 / 0.8492	0.7988
Minkowski and Nb = 1	0.9743 / 0.9047 / 0.9382	0.7237 / 0.7797 / 0.7507	0.7106 / 0.6726 / 0.6911	0.7371 / 0.7678 / 0.7521	0.8639 / 0.8690 / 0.8664	0.7988
Minkowski and Nb = 3	0.9697 / 0.9523 / 0.9609	0.7633 / 0.7678 / 0.7655	0.7361 / 0.7142 / 0.7250	0.7307 / 0.7916 / 0.76	0.8695 / 0.8333 / 0.8510	0.8119
Minkowski and Nb = 5	0.9636 / 0.9464 / 0.9549	0.7927 / 0.7738 / 0.7831	0.7613/ 0.7023 / 0.7306	0.7157 / 0.8095 / 0.7597	0.8734 / 0.8630 / 0.8682	0.8190
Minkowski and Nb = 7	0.9634 / 0.9404 / 0.9518	0.7572 / 0.7797 / 0.7683	0.7516 / 0.7023 / 0.7261	0.7311 / 0.8095 / 0.7683	0.8812 / 0.8392 / 0.8597	0.8143
Minkowski and Nb = 9	0.9461 / 0.9404 / 0.9432	0.7485 / 0.7440 / 0.7462	0.7134 / 0.6964 / 0.7048	0.7189 / 0.7916 / 0.7535	0.8789 / 0.8214 / 0.8492	0.7988

Table 10. : SVM classifier performance using distinct configurations and HTFT+STAT input features

SVM Configuration	Precision/Recall/ F1-score(Healthy rotor)	Precision/Recall/ F1-score(1BB)	Precision/Recall/ F1-score(2BB)	Precision/Recall/ F1-score(3BB)	Precision/Recall/ F1-score(4BB)	**Accuracy**
C = 1 and g = 0.0025	0.9733 / 0.4345 / 0.6008	0.3659 / 0.8690 / 0.5149	0.4947 / 0.2797 / 0.3574	0.7339 / 0.4761 / 0.5776	0.7469 / 0.7202 / 0.7333	0.5559
C = 1 and g = 0.25	0.9537 / 0.9821 / 0.9677	0.7622 / 0.7440 / 0.7530	0.5970 / 0.7142 / 0.6504	0.7635 / 0.6726 / 0.7151	0.8506 / 0.7797 / 0.8136	0.7785
C = 1 and g = 0.50	0.9422 / 0.9702 / 0.9560	0.7485 / 0.7440 / 0.7462	0.6647/ 0.6964 / 0.6802	0.7711 / 0.7619 / 0.7664	0.8734 / 0.8214 / 0.8466	0.7988
C = 100 and g = 0.0025	0.9485 / 0.9880 / 0.9679	0.5541 / 0.7916 / 0.6519	0.4782 / 0.4583 / 0.4680	0.767 / 0.4702 / 0.583	0.795 / 0.7619 / 0.7781	0.694
C = 100 and g = 0.25	0.9878 / 0.9642 / 0.9759	0.841 / 0.7559 / 0.7962	0.7458 / 0.8035 / 0.7736	0.783 / 0.8809 / 0.8291	0.8967 / 0.8273 / 0.8607	0.8464
C = 100 and g = 0.50	0.9699 / 0.9583 / 0.9640	0.817/ 0.744 / 0.7788	0.7329 / 0.7678 / 0.75	0.7945 / 0.875 / 0.8328	0.906 / 0.863 / 0.8841	0.8416
C = 200 and g = 0.0025	0.9593 / 0.9821 / 0.9705	0.5826 / 0.7976 / 0.6733	0.4942 / 0.5119 / 0.5029	0.77 / 0.4583 / 0.5746	0.7865 / 0.7678 / 0.777	0.7035
C = 200 and g = 0.25	0.9818 / 0.9642 / 0.9729	0.8193 / 0.756 / 0.7863	0.7237 / 0.7797 / 0.7507	0.7868 / 0.8571 / 0.8205	0.8846 / 0.8214 / 0.8518	0.8357
C = 200 and g = 0.50	0.9698 / 0.9583 / 0.964	0.7961 / 0.7440 / 0.7692	0.7192 / 0.7321 / 0.7256	0.7736 / 0.875 / 0.8212	0.9038 / 0.8392 / 0.8703	0.8297
C = 300 and g = 0.0025	0.9482 / 0.9821 / 0.9649	0.5826 / 0.7976 / 0.6733	0.5058 / 0.5178 / 0.5117	0.76 / 0.4523 / 0.5671	0.7926 / 0.7738 / 0.7831	0.7047
C = 300 and g = 0.25	0.9757 / 0.9583 / 0.967	0.8089 / 0.7559 / 0.7815	0.715 / 0.7619 / 0.7377	0.7826 / 0.8571 / 0.8181	0.8903 / 0.8214 / 0.8544	0.8309
C = 300 and g = 0.50	0.964 / 0.9583 / 0.9611	0.7888 / 0.7559 / 0.772	0.730 / 0.7083 / 0.719	0.7668 / 0.8809 / 0.8199	0.8974 / 0.8333 / 0.8641	0.8273

Table 11. : Comparison between the best accuracy results using or not PCC

Number of features	SVM parameters	Accuracy
20 (No-PCC)	C = 100 / g = 0.25	0.8464
10 (PCC)	C = 100 / g = 0.50	0.8274

duced number of features using PCC is capable of evaluate the rotor structure with the same effectiveness as the case with 20 features. Therefore, the severity of a failure, for example, can be investigated using 10 features instead of 20.

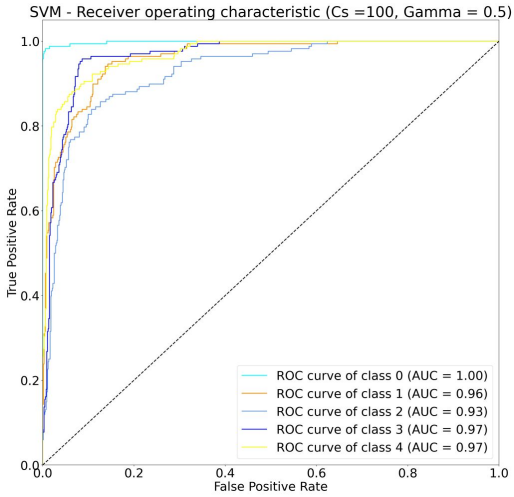

Fig. 6: ROC curves for SVM classifier and features after applying PCC (C = 100 and g = 0.50)

7. CONCLUSION

This paper presents a wide experimental comparison between some important signal processing techniques used for fault diagnosis in rotating electrical machines and some common machine learning methods also used in this field, for broken rotor bars detection and/or classification.In addition, the present study has proposed a relevant approach using only data for a induction motor running at very low slip, since this operational condition is particularly adverse for broken rotor bars detection using the traditional method MCSA. It was clear that the use of Hilbert and FFT techniques is capable of extract more insightful information about the rotor condition using the stator current as data source. Although FFT and SVM, as shown in the results (Figures 10, 11 and Table 8), have demonstrated good results, the use of HT+STAT features have clearly indicated best accuracy values. However, the classifier parameters, as noted in all cases, must be carefully chosen, in order to avoid false positive and false negative alarms. The present work has also evaluated the use of Pearson correlation coefficient to select stator current features and the results has proven the capacity of maintain a good accuracy using a reduced number of inputs. Therefore, the main contributions of this paper can be summarized as follows:
i-) ability to use several classifiers by combining distinct parameters in this kind of technical problem;
ii-) possibility to apply the present approach for an induction motor running at very low slip condition (close to 1%). The rated slip of the tested motor is 3.4%;
iii-) it is possible to classify the damaged rotor severity for a motor fed by an inverter;
iv-) possibility do identify not only a fault, but its severity with a good accuracy;
v-) the proposed study allows the use of a reduced number of input features, combining frequency domain and statistical features.
Further investigations should be conducted to evaluate the rotor faults at variable speeds and using distinct feature reduced methods.In addition, the authors are carrying out new studies using other types of digital signal processing for performing better feature extraction.

8. ACKNOWLEDGMENTS

The authors thank the Sao Pauo Research Foundation (FAPESP) under grants 2016/02525-1 and 2018/05214-2 for the financial support and Nove de Julho University to provide laboratory apparatus support.

9. REFERENCES

[1] I. L. Sauer, H. Tatizawa, F. A. Salotti, and S. S. Mercedes, "A comparative assessment of Brazilian electric motors performance with minimum efficiency standards," *Renew. Sustain. Energy Rev.*, vol. 41, pp. 308–318, jan 2015. [Online]. Available: http://dx.doi.org/10.1016/j.rser.2014.08.053https://linkinghub.elsevier.com/retrieve/pii/S1364032114007291

[2] H. Chen, B. Jiang, and N. Lu, "A multi-mode incipient sensor fault detection and diagnosis method for electrical traction systems," *International Journal of Control, Automation and Systems*, 2018.

[3] A. E. Treml, R. A. Flauzino, and G. C. Brito, "Emd and mcsa improved via hilbert transform analysis on asynchronous machines for broken bar detection using vibration analysis," in *2019 IEEE Milan PowerTech*, 2019, pp. 1–6.

[4] X. Liang and K. Edomwandekhoe, "Condition monitoring techniques for induction motors," in *2017 IEEE Ind. Appl. Soc. Annu. Meet.* IEEE, oct 2017, pp. 1–10. [Online]. Available: http://ieeexplore.ieee.org/document/8101860/

[5] C. G. Dias and F. H. Pereira, "Broken Rotor Bars Detection in Induction Motors Running at Very Low Slip Using a Hall Effect Sensor," *IEEE Sens. J.*, vol. 18, no. 11, pp. 4602–4613, jun 2018. [Online]. Available: https://ieeexplore.ieee.org/document/8338052/

[6] R. Puche-Panadero, M. Pineda-Sanchez, M. Riera-Guasp, J. Roger-Folch, E. Hurtado-Perez, and J. Perez-Cruz, "Improved Resolution of the MCSA Method Via Hilbert Transform, Enabling the Diagnosis of Rotor Asymmetries at Very Low Slip," *IEEE Trans. Energy Convers.*, vol. 24, no. 1, pp. 52–59, mar 2009. [Online]. Available: http://ieeexplore.ieee.org/document/4749311/

[7] B. Xu, L. Sun, L. Xu, and G. Xu, "Improvement of the Hilbert Method via ESPRIT for Detecting Rotor Fault in Induction Motors at Low Slip," *IEEE Trans. Energy Convers.*, vol. 28, no. 1, pp. 225–233, mar 2013. [Online]. Available: http://ieeexplore.ieee.org/document/6407981/

[8] P. Gangsar and R. Tiwari, "Signal based condition monitoring techniques for fault detection and diagnosis of induction motors: A state-of-the-art review," *Mechanical Systems and Signal Processing*, vol. 144, p. 106908, 2020.

[Online]. Available: http://www.sciencedirect.com/science/article/pii/S0888327020302946

[9] J. Rangel-Magdaleno, H. Peregrina-Barreto, J. Ramirez-Cortes, and I. Cruz-Vega, "Hilbert spectrum analysis of induction motors for the detection of incipient broken rotor bars," *Measurement*, vol. 109, pp. 247 – 255, 2017.

[10] R. Puche-Panadero, J. Martinez-Roman, A. Sapena-Bano, J. Burriel-Valencia, M. Pineda-Sanchez, J. Perez-Cruz, and M. Riera-Guasp, "New method for spectral leakage reduction in the fft of stator currents: Application to the diagnosis of bar breakages in cage motors working at very low slip," *IEEE Transactions on Instrumentation and Measurement*, vol. 70, pp. 1–11, 2021.

[11] D. Cleber-Gustavo, S. Luiz-Carlos, and C. Ivan-Eduardo, "Fuzzy-based statistical feature extraction for detecting broken rotor bars in line-fed and inverter-fed induction motors," *Energies*, vol. 12, no. 2381, pp. 1–29, June 2019.

[12] I. Martin-Diaz, D. Morinigo-Sotelo, O. Duque-Perez, and R. D. J. Romero-Troncoso, "Advances in Classifier Evaluation: Novel Insights for an Electric Data-Driven Motor Diagnosis," *IEEE Access*, vol. 4, pp. 7028–7038, 2016.

[13] J. Chen, J. Jiang, X. Guo, and L. Tan, "An efficient cnn with tunable input-size for bearing fault diagnosis," *International Journal of Computational Intelligence Systems*, vol. 14, pp. 625–634, 2021. [Online]. Available: https://doi.org/10.2991/ijcis.d.210113.001

[14] N. Truong, T. Seo, and S. Nguyen, "Bearing fault online identification based on anfis," *International Journal of Control, Automation and Systems*, 2021.

[15] P. A. Delgado-Arredondo, D. Morinigo-Sotelo, R. A. Osornio-Rios, J. G. Avina-Cervantes, H. Rostro-Gonzalez, and R. de Jesus Romero-Troncoso, "Methodology for fault detection in induction motors via sound and vibration signals," *Mechanical Systems and Signal Processing*, vol. 83, pp. 568 – 589, 2017.

[16] T. P. Carvalho, F. A. Soares, R. Vita, R. da P. Francisco, J. P. Basto, and S. G. Alcalá, "A systematic literature review of machine learning methods applied to predictive maintenance," *Computers and Industrial Engineering*, vol. 137, pp. 1–10, 2019.

[17] J. Burriel-Valencia, R. Puche-Panadero, A. Sapena-Bano, M. Pineda-Sanchez, and J. Martinez-Roman, "Cost-effective reduced envelope of the stator current via synchronous sampling for the diagnosis of rotor asymmetries in induction machines working at very low slip," *Sensors*, vol. 19, no. 3471, pp. 1–16, Aug. 2019.

[18] A. Naha, A. K. Samanta, A. Routray, and A. K. Deb, "A Method for Detecting Half-Broken Rotor Bar in Lightly Loaded Induction Motors Using Current," *IEEE Trans. Instrum. Meas.*, vol. 65, no. 7, pp. 1614–1625, jul 2016. [Online]. Available: http://ieeexplore.ieee.org/document/7450652/

[19] A. Sapena-Bano, M. Pineda-Sanchez, R. Puche-Panadero, J. Martinez-Roman, and Ž. Kanović, "Low-cost diagnosis of rotor asymmetries in induction machines working at a very low slip using the reduced envelope of the stator current," *IEEE Transactions on Energy Conversion*, vol. 30, no. 4, pp. 1409–1419, Dec. 2015.

[20] D. Shi, P. Unsworth, and R. Gao, "Sensorless Speed Measurement of Induction Motor Using Hilbert Transform and Interpolated Fast Fourier Transform," *IEEE Trans. Instrum. Meas.*, vol. 55, no. 1, pp. 290–299, 2006. [Online]. Available: http://ieeexplore.ieee.org/lpdocs/epic03/wrapper.htm?arnumber=1583893

[21] W. Laala, S. Guedini, and S. Zouzou, "Novel approach for diagnosis and detection of broken bar in induction motor at low slip using fuzzy logic," in *8th IEEE Symposium on Diagnostics for Electrical Machines, Power Electronics Drives*, 2011, pp. 511–516.

[22] M. Fernandez-Temprano, P. E. Gardel-Sotomayor, O. Duque-Perez, and D. Morinigo-Sotelo, "Broken bar condition monitoring of an induction motor under different supplies using a linear discriminant analysis," in *2013 9th IEEE Int. Symp. Diagnostics Electr. Mach. Power Electron. Drives*. IEEE, aug 2013, pp. 162–168. [Online]. Available: http://ieeexplore.ieee.org/document/6645712/

[23] T. Yang, H. Pen, Z. Wang, and C. S. Chang, "Feature Knowledge Based Fault Detection of Induction Motors Through the Analysis of Stator Current Data," vol. 65, no. 3, pp. 549–558, 2016.

[24] B. Godsey, *Think Like a Data Scientist: Tackle the Data Science Process Step-by-Step*, 1st ed. USA: Manning Publications Co., 2017.

[25] I. Martin-Diaz, D. Morinigo-Sotelo, O. Duque-Perez, and R. D. J. Romero-Troncoso, "Advances in classifier evaluation: Novel insights for an electric data-driven motor diagnosis," *IEEE Access*, vol. 4, pp. 7028–7038, 2016.

[26] Y. Lei, *Intelligent Fault Diagnosis and Remaining Useful Life Prediction of Rotating Machinery*, 1st ed. Butterworth-Heinemann, 2017.

[27] L. Kong and H. Nian, "Fault detection and location method for mesh-type dc microgrid using pearson correlation coefficient," *IEEE Transactions on Power Delivery*, pp. 1–1, 2020.

[28] J. Ge, T. Niu, D. Xu, G. Yin, and Y. Wang, "A rolling bearing fault diagnosis method based on eemd-wsst signal reconstruction and multi-scale entropy," *Entropy*, vol. 22, no. 3, 2020. [Online]. Available: https://www.mdpi.com/1099-4300/22/3/290